Int. J. Solids Structures Vol. 29, No. 10, pp. 1241–1253, 1992
Printed in Great Britain.

0020–7683/92 $5.00+.00

ON THE STABILITY AND POST-CRITICAL BEHAVIOR OF ELASTIC STRUCTURES WITH DRY FRICTION

Z. MRÓZ
Institute of Fundamental Technological Research, Polish Academy of Sciences, Swiętokrzyska 21, PL 00-049 Warsaw, Poland

and

R. H. PLAUT
Charles E. Via, Jr. Department of Civil Engineering, Virginia Polytechnic Institute and State University, Blacksburg, VA 24061, U.S.A.

(*Received* 4 *March* 1991; *in revised form* 20 *September* 1991)

Abstract—The stability of discrete elastic systems subjected to conservative loading is governed by the potential energy, which is a function of the generalized coordinates. When dry friction is present, it affects the stability conditions and the post-critical response. Quasi-static loading is considered and the normal forces to the friction surface are assumed to be specified. General critical state conditions are obtained in terms of the potential energy and the dissipation function. Then several examples are presented to illustrate various types of behavior. It is seen that limit points, bifurcation points, and transition points (associated with slip activation or deactivation) may occur on the deformation path, and that a sudden "snap" from one state to another is a common phenomenon when the system includes dry friction.

1. INTRODUCTION

This paper is concerned with the deformation response and stability of discrete elastic structures in which dry friction is present. The friction forces may act at structural interactions with foundations, or in connections or hinges between structural components. They are associated with contact slip and in general provide a non-conservative action on the system.

Under quasi-static loading, the introduction of dry friction into an elastic system may change the stability and post-critical behavior drastically. For example, an elastic system may reach a bifurcation point and then deform smoothly along a stable post-buckling path, whereas dry friction may eliminate this critical point and may introduce new ones, often leading to a snap-through type of instability. This effect of dry friction is in contrast to that of viscous damping, which depends on velocities and does not alter the static deformation behavior of conservative non-gyroscopic systems.

The modeling of friction is not a simple matter [e.g. see Oden and Martins (1985) and Martins *et al.* (1990)]. The Coulomb damping model has been used in many analyses of the dynamic response of structures [e.g. Pierre *et al.* (1985)]. If the normal forces on the contact boundary are assumed to be known, then the friction forces are derivable from a dissipation function and the formalism of plasticity theory can be applied [see Michałowski and Mróz (1978) and section 4.3 of Oden and Martins (1985)]. This approach is used here.

In the following section, equilibrium equations and general stability conditions are obtained in terms of the potential energy and the dissipation function. Several types of critical states are described. Then, in Sections 3–6, four examples are presented to demonstrate these critical states and the effect of dry friction on stability and post-critical behavior.

2. STABILITY OF ELASTIC SYSTEMS WITH FRICTION

Consider a discrete elastic system that contains some friction elements. First, suppose that the friction elements are not active, and that the system then has n generalized coordinates q_i, $i = 1, 2, \ldots, n$, a load parameter λ, and the potential energy function $V(q_i, \lambda)$.

The equilibrium equations are obtained by requiring the stationarity of V with respect to q_i, i.e.

$$\frac{\partial V}{\partial q_i} \equiv V_i(q_j, \lambda) = 0, \quad i = 1, 2, \ldots, n. \tag{1}$$

The incremental equilibrium equations are generated from eqn (1), namely

$$V_{ij}\dot{q}_j + V_{i\lambda}\dot{\lambda} = 0, \quad i = 1, 2, \ldots, n, \tag{2}$$

where $\dot{q}_j$ and $\dot{\lambda}$ denote increments or rates with respect to some parameter, the subscripts i, j and λ indicate partial differentiation with respect to q_i, q_j and λ, respectively, and a repeated subscript implies summation. The equilibrium state is stable if $\{V_{ij}\}$ is positive definite.

The deformation process reaches a critical point when the tangent stiffness matrix becomes singular, that is, when

$$V_{ij}t_j = 0, \quad t_j \neq 0, \det V_{ij} = 0, \tag{3}$$

where $\{t_j\}$ is the eigenvector. A limit point occurs when $\dot{\lambda} = 0$ and $V_{i\lambda}t_i \neq 0$, whereas the normality condition $V_{i\lambda}t_i = 0$ is satisfied at a bifurcation point (Thompson and Hunt, 1973; Huseyin, 1975).

Now assume that the friction elements are active. Their actions will be represented by friction forces associated with instantaneous slips of these elements. Let a_k and $\dot{a}_k$, $k = 1, 2, \ldots, m$, denote the displacements and rates (or slips), respectively, of the friction elements. Assume that there are now $\bar{n}$ generalized coordinates q_i, $i = 1, 2, \ldots, \bar{n}$, and that the a_k can be written in terms of them, i.e.

$$a_k = a_k(q_i), \quad k = 1, 2, \ldots, m, \quad i = 1, 2, \ldots, \bar{n}. \tag{4}$$

The description of frictional slip here follows the formalism of plasticity theory [see Michałowski and Mróz (1978)]. Let T_1 and T_2 denote the tangential force components, and N the normal force component, at the contact surface with respect to a Cartesian reference system. The limit friction condition can be written as follows:

$$F(T_1, T_2, N) \equiv f(T_1, T_2) - \mu N \leqslant 0, \tag{5}$$

where μ is a coefficient of friction and the normal force is assumed to be positive when it is compressive.

Consider the case of a slip rule of the form

$$\dot{a}_1 = \dot{a}\frac{\partial f}{\partial T_1}, \quad \dot{a}_2 = \dot{a}\frac{\partial f}{\partial T_2}, \quad \dot{a}_n = 0, \quad \dot{a} \geqslant 0, \quad \text{for} \quad F = \dot{F} = 0,$$

$$\dot{a}_1 = \dot{a}_2 = \dot{a}_n = 0, \quad \text{for} \quad F < 0 \quad \text{or} \quad F = 0, \quad \dot{F} < 0, \tag{6}$$

where

$$\dot{a} = (\dot{a}_1^2 + \dot{a}_2^2)^{1/2}. \tag{7}$$

This slip rule preserves the normality of slips to the limit surface (5) only in the plane N = constant, as there is no normal slip component. To preserve the normality property, the following analysis will be confined to cases where normal forces on contact surfaces are specified from static equilibrium conditions and it is sufficient to consider intersections of the limit surface (5) by planes N = constant, so that eqn (5) becomes

$$F(T_1, T_2, T_0) \equiv f(T_1, T_2) - T_0 = 0, \quad T_0 = \mu N, \tag{8}$$

and T_0 is specified at each contact point.

The dissipation function

$$D = T_i \dot{a}_i \tag{9}$$

is introduced. It is a homogeneous function of slips of degree one. If there is a single friction element, then

$$D = D(\dot{a}_1, \dot{a}_2) = T_1 \dot{a}_1 + T_2 \dot{a}_2 \tag{10}$$

and the inverse relation to eqn (6) takes the form

$$T_1 = \frac{\partial D}{\partial \dot{a}_1}, \quad T_2 = \frac{\partial D}{\partial \dot{a}_2}, \tag{11}$$

when D is differentiable, i.e. when $(\dot{a}_1, \dot{a}_2) \neq (0, 0)$. For the case of isotropic friction,

$$F(T_1, T_2, T_0) \equiv (T_1^2 + T_2^2)^{1/2} - T_0 = 0, \quad D = T_0(\dot{a}_1^2 + \dot{a}_2^2)^{1/2}, \tag{12}$$

so that eqns (11) become

$$T_1 = T_0 \dot{a}_1/\dot{a}, \quad T_2 = T_0 \dot{a}_2/\dot{a}, \tag{13}$$

where $\dot{a}$ is defined in eqn (7). When eqn (5) is satisfied as an inequality, $F < 0$, there is no slip at the friction element and the friction force is represented in the force plane by an interior point of the domain enclosed by $F = 0$.

With the use of eqn (4), the dissipation function D given by eqn (9) can be expressed in terms of $\dot{q}_i$ and q_i, $i = 1, 2, \ldots, \bar{n}$, namely (when $\dot{a}_1 \neq 0$ and $\dot{a}_2 \neq 0$)

$$D = T_i \frac{\partial a_i}{\partial q_j} \dot{q}_j = \frac{\partial D}{\partial \dot{a}_i} \frac{\partial \dot{a}_i}{\partial \dot{q}_j} \dot{q}_j = \frac{\partial D}{\partial \dot{q}_j} \dot{q}_j = \bar{T}_j \dot{q}_j \tag{14}$$

where the dissipation forces $\bar{T}_j$ are given by

$$\bar{T}_j = \frac{\partial D}{\partial \dot{q}_j}(q_i, \dot{q}_i). \tag{15}$$

Then the potential energy $V = V(q_i, \lambda)$ and the dissipation function $D = D(q_i, \dot{q}_i)$ can be used to generate equilibrium and stability conditions. Accounting for dissipative forces, the equilibrium equations are

$$\frac{\partial V}{\partial q_i} + \frac{\partial D}{\partial \dot{q}_i} = 0, \quad \text{i.e. } V_i + D_{(i)} = 0, \quad i = 1, 2, \ldots, \bar{n}, \tag{16}$$

where the notation $D_{(i)} = \partial D/\partial \dot{q}_i$ is used.

Now consider the incremental equilibrium equations along any deformation path in the configuration space, $q_i = q_i(s)$, $\lambda = \lambda(s)$, where s denotes the arc length. Departing from the equilibrium position at $s = s_0$, one can write

$$q_i(s)-q_i(s_0) = (s-s_0)\dot{q}_i+(s-s_0)^2\ddot{q}_i/2+\cdots,$$
$$\lambda(s)-\lambda(s_0) = (s-s_0)\dot{\lambda}+(s-s_0)^2\ddot{\lambda}/2+\cdots. \tag{17}$$

Differentiating eqn (16) and retaining linear terms in $s-s_0$, one obtains

$$V_{ij}\dot{q}_j+D_{(ij)}\dot{q}_j+D_{(ij)}\ddot{q}_j+V_{i\lambda}\dot{\lambda} = 0, \quad i = 1,2,\ldots,\bar{n}, \tag{18}$$

where

$$V_{ij} = \frac{\partial^2 V}{\partial q_i \partial q_j}, \quad D_{(i)j} = \frac{\partial^2 D}{\partial \dot{q}_i \partial q_j}, \quad D_{(ij)} = \frac{\partial^2 D}{\partial \dot{q}_i \partial \dot{q}_j}, \quad V_{i\lambda} = \frac{\partial^2 V}{\partial q_i \partial \lambda}. \tag{19}$$

Equations (18) constitute the incremental equilibrium equations. Let us note that D is a homogeneous function of $\dot{q}_i$ of degree one. Hence $D_{(i)}$ and $D_{(i)j}$ are homogeneous functions of $\dot{q}_i$ of degree zero, and $D_{(ij)}$ is homogeneous of degree minus one. In view of Euler's theorem for homogeneous functions, the following equalities can be stated:

$$D_{(i)j}\dot{q}_i = \frac{\partial}{\partial q_j}\left(\frac{\partial D}{\partial \dot{q}_i}\right)\dot{q}_i = \frac{\partial}{\partial q_j}\left(\frac{\partial D}{\partial \dot{q}_i}\dot{q}_i\right) = \frac{\partial D}{\partial q_j} = D_j,$$
$$D_{(ij)}\dot{q}_i = \frac{\partial}{\partial \dot{q}_i}\left(\frac{\partial D}{\partial \dot{q}_j}\right)\dot{q}_i = D_{(ij)}\dot{q}_j = 0. \tag{20}$$

From eqn (20) it follows that $D_{(ij)}$ is a singular matrix and $\dot{q}_i$ is its eigenvector. Multiplying eqn (18) by $\dot{q}_i$ and using eqn (20), one obtains

$$(V_{ij}+D_{(ij)})\dot{q}_i\dot{q}_j+V_{i\lambda}\dot{q}_i\dot{\lambda} = V_{ij}\dot{q}_i\dot{q}_j+D_j\dot{q}_j+V_{i\lambda}\dot{q}_i\dot{\lambda} = 0. \tag{21}$$

Along the deformation path, several types of critical points are possible, such as limit points, transition points or bifurcation points. At a limit point, the path exhibits a local maximum [Fig. 1(a)] or a local minimum [Fig. 1(b)], slip continues in all active elements, and one has

$$(V_{ij}+D_{(ij)})\dot{q}_i\dot{q}_j = V_{ij}\dot{q}_i\dot{q}_j+D_j\dot{q}_j = 0, \quad \dot{\lambda} = 0, \quad V_{i\lambda}\dot{q}_i \neq 0. \tag{22}$$

A transition point is associated with slip activation or slip deactivation, and there is a slope discontinuity in the load–displacement curve, as illustrated for one type of case in Fig. 1(c). For example, if only elastic deformation occurs for $s < s_0$ and if slip is activated at $s = s_0$, then eqns (2) govern for $s < s_0$ and eqns (18) apply as s increases past s_0, and the transition from stable to unstable response at $s = s_0$ occurs when

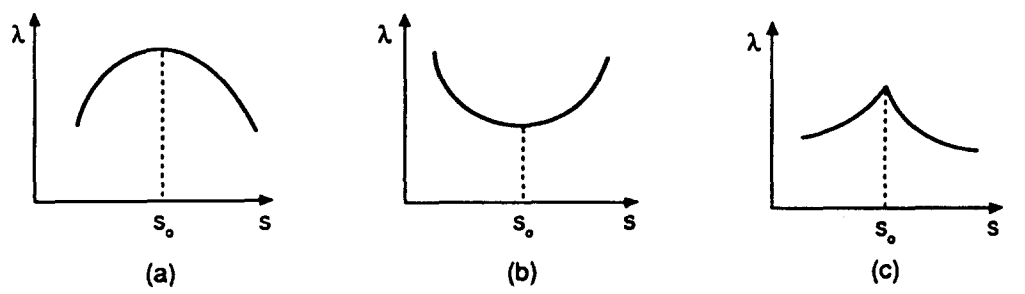

Fig. 1. Limit points (a, b) and transition point (c) on load–displacement curve.

$$V_{ij}\dot{q}_i^-\dot{q}_j^- > 0, \quad V_{ij}\dot{q}_i^+\dot{q}_j^+ + D_j\dot{q}_j^+ < 0 \tag{23}$$

where $\dot{q}_i^-$ and $\dot{q}_i^+$ denote values for $s = s_0^-$ and $s = s_0^+$, respectively, at the transition point. If slip occurs and the state q_i is stable, then

$$V_{ij}\dot{q}_i\dot{q}_j + D_j\dot{q}_j > 0. \tag{24}$$

Bifurcation may occur when

$$V_{ij}\dot{t}_i = 0, \quad [V_{ij} + D_{(ij)}]\dot{t}_j = 0, \quad i = 1, 2, \ldots, \bar{n}, \tag{25}$$

where $\{\dot{t}_j\}$ is an eigenvector. However, since $D_{(ij)}$ is in general a non-linear matrix of slips of degree zero, the resulting eigenvalue problem may be non-linear. It turns out that the friction effect tends to eliminate the bifurcation points which would have existed in a purely elastic system, and typically induces the appearance of limit points or transition points and the occurrence of a "snap" instability.

3. EXAMPLE 1: RIGID BAR ON FRICTIONAL FOUNDATION

Consider a rigid bar of length L (Fig. 2). Its base is pinned with an elastic rotational spring of stiffness c. A vertical load P is applied at the tip of the bar. The bar rests on a frictional foundation coinciding with the plane of the figure, and the specific friction force (per unit length of the bar) is q. The angular coordinate θ is measured from the vertical [Fig. 2(b)], and the initial configuration (when the spring is unstretched and before slip has been activated) is $\theta = \delta$ [Fig. 2(a)].

The bar does not displace until slip is activated, and then $\bar{n} = m = 1$ and

$$\begin{aligned} &q_1 = \theta, \quad a_1 = (L/2)\theta, \quad T_1 = qL, \quad \lambda = P, \\ &V = (c/2)(\theta-\delta)^2 - PL(\cos\delta - \cos\theta), \quad D = T_1\dot{a}_1 = qL^2\dot{\theta}/2. \end{aligned} \tag{26}$$

The equilibrium equation (16) becomes

$$c(\theta-\delta) - PL\sin\theta + qL^2/2 = 0. \tag{27}$$

In terms of the quantities

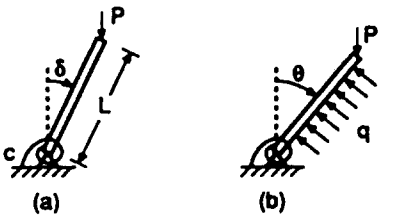

Fig. 2. Geometry of Example 1: (a) before slip; (b) during slip.

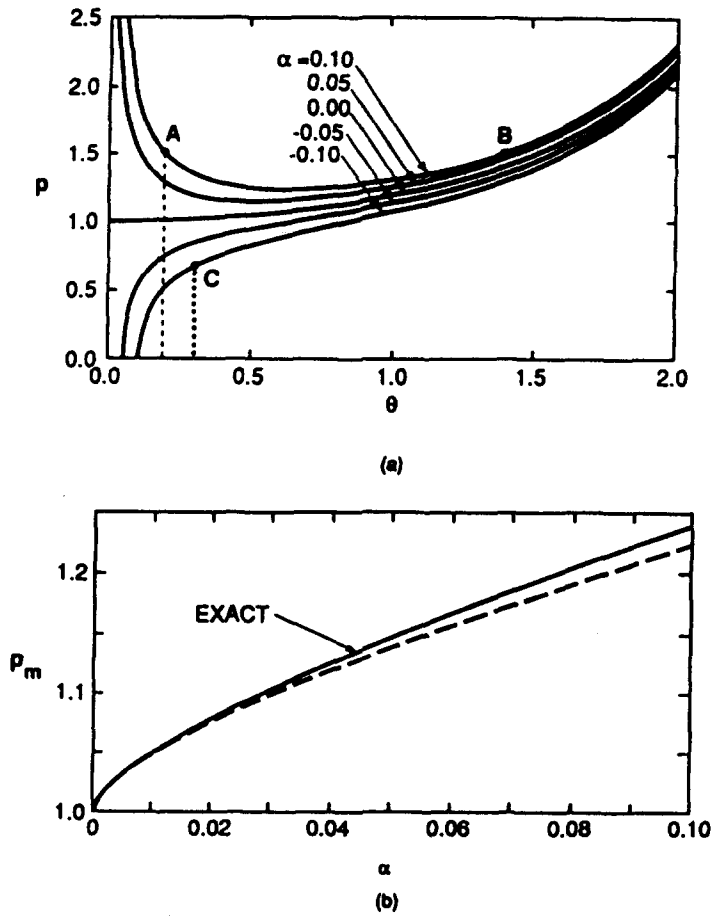

Fig. 3. Example 1: (a) load-displacement curves; (b) minimum load.

$$p = PL/c, \quad \bar{q} = qL^2/(2c), \quad \alpha = \bar{q} - \delta, \tag{28}$$

the solutions of eqn (27) for $0 \leqslant \theta \leqslant 2$ are plotted as solid curves in Fig. 3(a) for $\alpha = 0.10$, 0.05, 0, -0.05 and -0.10. The portions of the paths with positive slope are stable and those with negative slope (to the left of the minima) are unstable.

Conditions (22) for a limit point, along with eqn (27), yield

$$\tan\theta_m - \theta_m = \alpha, \quad p_m = \frac{1}{\cos\theta_m} \cong 1 + \frac{1}{2}(3\alpha)^{2/3}, \tag{29}$$

where θ_m and p_m denote the values of θ and p, respectively, at the limit points, which are at the minima. For small positive values of α, it is seen that the limit points exhibit the typical sensitivity with respect to α of 2/3 order. The variation of p_m with α is shown in Fig. 3(b), where the solid curve gives the exact result and the dashed curve is based on the approximate relation for small α.

First, assume that the unloaded bar is vertical, so that $\delta = 0$ and $\alpha \geqslant 0$. If $\alpha = 0$ (no friction), symmetric bifurcation occurs at the critical point $p = 1$ and the post-critical response $p = \theta/\sin\theta$ is stable. If friction is present, so that $\alpha > 0$, there is no bifurcation from the trivial solution $\theta = 0$ and the vertical bar is stable for all values of p (i.e. the "critical load" is infinite).

Now assume $\delta > 0$. Slip is activated when $\theta = \delta$ in eqn (27), i.e. when p reaches the value $p^* = q/\sin\delta$. For example, if $\delta = 0.20$ and $q = 0.30$, then $\alpha = 0.10$ and $p^* = 1.51$, so that as the load is increased, the bar remains at $\theta = \delta$ until p reaches the value 1.51 [dashed line in Fig. 3(a)], then slip is activated [point A in Fig. 3(a)], then the bar exhibits a dynamic

"snap" to the configuration $\theta = 1.39$ at point B [which also satisfies eqn (27) at $p = 1.51$], and finally θ increases smoothly with further increase in the load. As another example, assume $\delta = 0.30$ and $q = 0.20$. Then $\alpha = -0.10$ and $p^* = 0.68$. As the load is increased, the system follows the vertical dotted line in Fig. 3(a) until $p = p^*$ (point C) and then θ increases along the stable rising path, with no snap occurring in this case when slip is activated.

Similar curves to those in Fig. 3(a) were obtained by Kerr (1973) in a model of vertical buckling of a railroad track under compression. The model involved rigid bars, rotational springs and a conservative distributed load (whereas the friction force here is non-conservative). The vibrations of a rigid bar pinned at its base and subjected to other types of dry friction action were examined by Hoff (1949) and Klepp (1990).

4. EXAMPLE 2: RIGID BAR WITH STRING

This model is similar to Example 1, but the frictional foundation is replaced by a friction element that is attached to the tip of the bar with a taut string of length b. The configuration before slip, in which the string is horizontal, is depicted in Fig. 4(a), while the displaced system is drawn in Fig. 4(b), where the angle of the string with the horizontal is denoted ϕ and the deflection components of the friction element are u_x and u_y, as shown. The horizontal and vertical components of the friction force acting on the element are denoted T_x and T_y, respectively.

After slip is activated, $\bar{n} = m = 2$ and

$$q_1 = \theta, \quad q_2 = \phi, \quad a_1 = u_x, \quad a_2 = u_y, \quad T_1 = T_x, \quad T_2 = T_y, \quad \lambda = P. \tag{30}$$

The limit friction condition is given by the first of eqns (12), and the slip rule

$$\dot{u}_x/\dot{u}_y = T_x/T_y \tag{31}$$

is obtained from eqns (13). From the geometry of Fig. 4, one can show that

$$\begin{aligned} u_x &= b + L\sin\theta - L\sin\delta - b\cos\phi, \\ u_y &= L\cos\delta - L\cos\theta - b\sin\phi, \end{aligned} \tag{32}$$

which leads to the incremental form

$$\dot{u}_x = L\dot{\theta}\cos\theta + b\dot{\phi}\sin\phi, \quad \dot{u}_y = L\dot{\theta}\sin\theta - b\dot{\phi}\cos\phi. \tag{33}$$

Equations (30) and (33) are used in eqn (10) to yield the dissipation function $D = D(\theta, \phi, \dot{\theta}, \dot{\phi})$, and the potential energy $V = V(\theta)$ is given in eqns (26).

From eqn (16), the equilibrium equations are given by

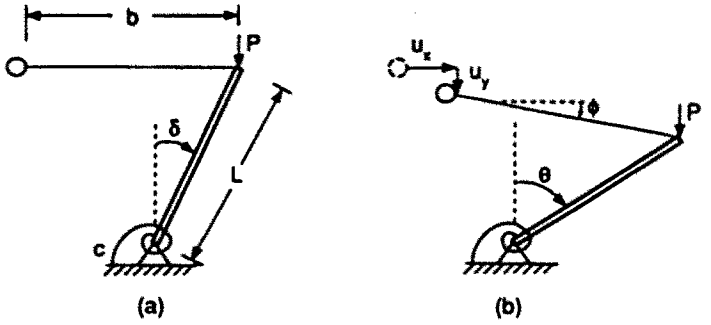

Fig. 4. Geometry of Example 2: (a) before slip; (b) during slip.

$$c(\theta-\delta)-PL\sin\theta+T_xL\cos\theta+T_yL\sin\theta=0 \tag{34}$$

and

$$(T_x\sin\phi-T_y\cos\phi)b=0. \tag{35}$$

With the use of eqn (35) in the first of eqns (12), one obtains

$$T_x=T_0\cos\phi,\quad T_y=T_0\sin\phi. \tag{36}$$

Then, if eqns (33) and (36) are substituted into eqn (31), one finds that

$$\dot{\phi}=(L/b)\dot{\theta}\sin(\theta-\phi). \tag{37}$$

Also, use of eqns (36) in the first partial derivatives of $D(\theta,\phi,\dot{\theta},\dot{\phi})$ yields

$$D_{(\theta)}=T_0L\cos(\theta-\phi),\quad D_{(\phi)}=0. \tag{38}$$

Differentiating D and V and utilizing eqns (36) and (37), condition (24) for stability becomes

$$\dot{\theta}^2\{c-PL\cos\theta-T_0L\sin(\theta-\phi)[1-(L/b)\sin(\theta-\phi)]\}>0. \tag{39}$$

If one substitutes eqns (36) into eqn (34), then determines the incremental form of the resulting equilibrium equation, and then uses eqn (37) to eliminate $\dot{\phi}$, one obtains

$$\dot{P}L\sin\theta=\dot{\theta}\{c-PL\cos\theta-T_0L\sin(\theta-\phi)[1-(L/b)\sin(\theta-\phi)]\}. \tag{40}$$

If $\sin\theta>0$, it follows from eqns (39) and (40) that the system is stable if $\dot{P}/\dot{\theta}>0$, i.e. if the load–displacement curve is rising.

Define the non-dimensional quantities

$$p=PL/c,\quad t_0=T_0L/c,\quad \beta=b/L. \tag{41}$$

When $t_0=0.1$ and $\beta=0.15$, results are plotted in Fig. 5 for initial angles $\delta=0.050$, 0.075 and 0.100. To determine when slip is activated, $\theta=\delta$ and $\phi=0$ are substituted into eqns (34) and (36), leading to $T_x=T_0$, $T_y=0$ and $P=T_0\cot\delta$. Therefore slip begins in Fig. 5

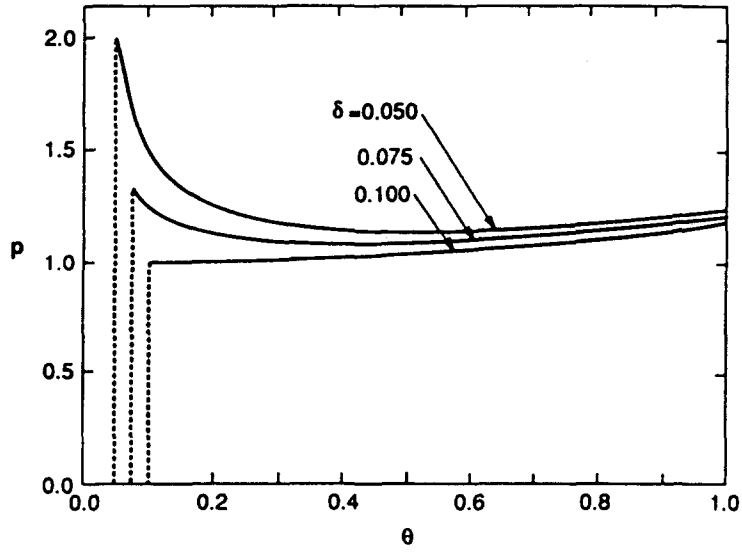

Fig. 5. Load–displacement curves for Example 2 when $t_0=0.1$ and $\beta=0.15$.

at $p = p^* = 1.998$, 1.331 and 0.997 for $\delta = 0.050$, 0.075 and 0.100, respectively. The subsequent load–displacement curves are computed incrementally with the use of eqn (40). If $\delta = 0.100$, the path is rising and stable, whereas the other two cases exhibit a dynamic snap to a large value of θ if p is increased beyond p^*.

5. EXAMPLE 3: RIGID BAR WITH TRANSLATIONAL SPRING

This example is the same as Example 2 except that the string is replaced by an elastic translational spring with stiffness k and unstretched length b. The unloaded configuration is depicted in Fig. 6(a). As the load P is increased quasi-statically from zero, elastic deformation occurs before slip is activated, so that the friction element does not move and $u_x = u_y = 0$, as shown in Fig. 6(b). Slip begins when P reaches a threshold value, and the configuration has the form sketched in Fig. 6(c).

Before slip is activated, $n = 1$, $q_1 = \theta$ and $\lambda = P$. Let η denote the deformed length of the spring. The potential energy is given by

$$V = (c/2)(\theta-\delta)^2 - PL(\cos\delta - \cos\theta) + (k/2)(\eta - b)^2 \tag{42}$$

where

$$\eta = (\eta_x^2+\eta_y^2)^{1/2}, \quad \eta_x = b + L\sin\theta - L\sin\delta - u_x,$$
$$\eta_y = L\cos\delta - L\cos\theta - u_y, \tag{43}$$

with $u_x = u_y = 0$. The equilibrium equation (1) becomes

$$c(\theta-\delta) - PL\sin\theta + kL[1-(b/\eta)](\eta_x\cos\theta + \eta_y\sin\theta) = 0. \tag{44}$$

If $\sin\theta > 0$, it turns out that the stability condition $V_{\theta\theta} > 0$ is satisfied if the load–displacement curve is rising.

It will be shown that the friction element begins to slip when the force $(\eta - b)k$ in the spring attains the value T_0, i.e. when

$$\eta = b + (T_0/k). \tag{45}$$

Hence the angle $\theta = \theta^*$ at slip activation can be computed by substituting eqn (45) and $u_x = u_y = 0$ into eqns (43), and the corresponding load $P = P^*$ can then be obtained from eqn (44).

When slip occurs, the system has three degrees of freedom: $n = 3$, $q_1 = \theta$, $q_2 = u_x$ and $q_3 = u_y$. The quantities a_1, a_2, T_1, T_2 and λ are the same as in eqns (30). The potential energy is given by eqn (42), and the dissipation function is

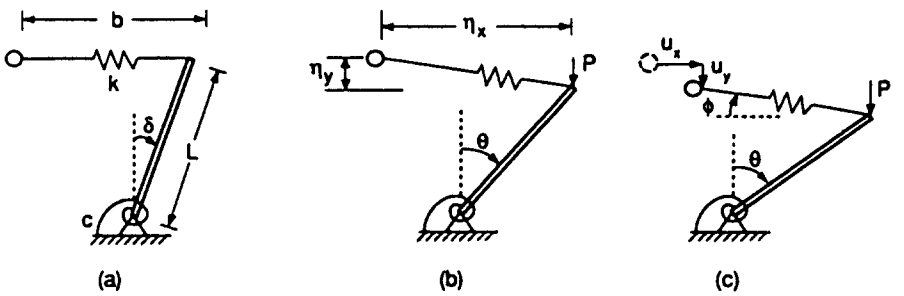

Fig. 6. Geometry of Example 3: (a) unloaded; (b) before slip; (c) during slip.

$$D = T_x\dot{u}_x + T_y\dot{u}_y. \tag{46}$$

From eqns (16), one obtains three equilibrium equations: eqn (44),

$$T_x = k\eta_x[1-(b/\eta)] \quad \text{and} \quad T_y = k\eta_y[1-(b/\eta)]. \tag{47}$$

Equation (45) then follows if eqns (47) are substituted into the limit friction condition in eqn (12).

Since the spring length η is constant when slip occurs, due to eqn (45), it is simpler to carry out the analysis in terms of the angles θ and ϕ, as in Example 2. From Fig. 6,

$$\eta_x = \eta\cos\phi, \quad \eta_y = \eta\sin\phi. \tag{48}$$

Using eqns (45) and (48), eqns (47) reduce to eqns (36) and the equilibrium equation (44) becomes

$$c(\theta-\delta) - PL\sin\theta + T_0L\cos(\theta-\phi) = 0. \tag{49}$$

With the use of eqns (43) and (48), one can show that $\dot{u}_x$ and $\dot{u}_y$ are given by eqns (33) with b replaced by η. Then, utilizing the slip rule (31) and eqns (45)–(48), it follows that eqns (36)–(40) are also valid in this example if b is replaced by η. Again, a rising load–displacement path is stable and a falling path is unstable if $0 < \theta < \pi$.

Results are presented in Figs 7 and 8 for $t_0 = 0.2$, $\beta = 0.1$ and $\gamma = 0.4$, where

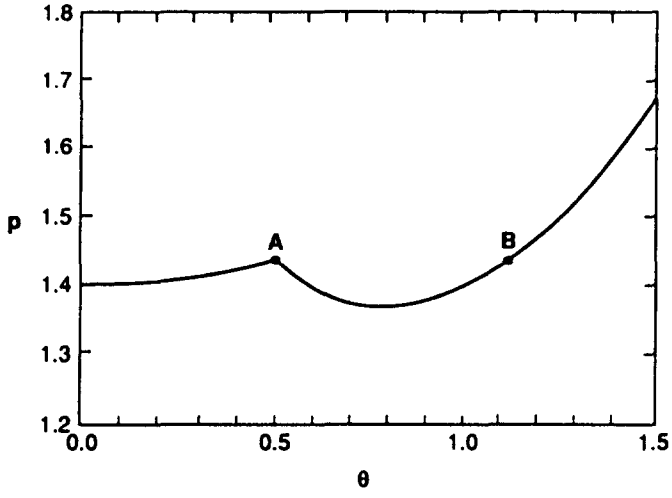

Fig. 7. Load–displacement curves for Example 3 when $t_0 = 0.2$, $\beta = 0.1$, $\gamma = 0.4$ and $\delta = 0$.

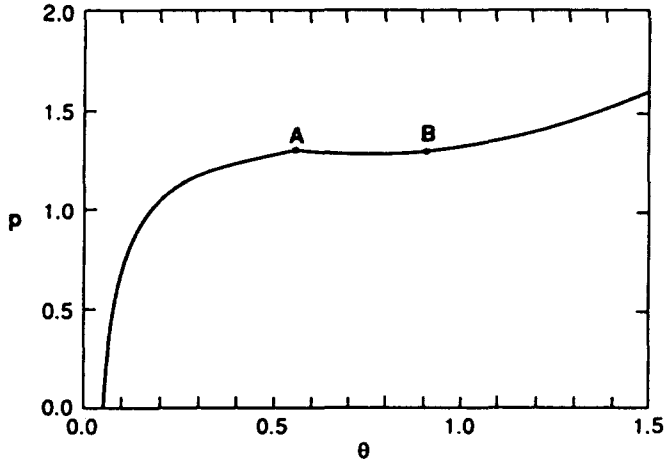

Fig. 8. Load–displacement curves for Example 3 when $t_0 = 0.2$, $\beta = 0.1$, $\gamma = 0.4$ and $\delta = 0.05$.

$$p = PL/c, \quad t_0 = T_0 L/c, \quad \beta = b/L, \quad \gamma = kL^2/c. \tag{50}$$

In Fig. 7, the unloaded bar is vertical, so that there is a trivial solution $\theta = 0$. Bifurcation occurs at $p = 1+\gamma = 1.4$, where $V_{\theta\theta} = 0$ (note that the ordinate in Fig. 7 does not start at $p = 0$). The stable, elastic post-buckling path is determined from eqn (44). Slip is activated when eqn (45) is satisfied, which occurs at $p = 1.44$ with $\theta = 0.51$ and $\phi = 0.21$ (point A). The subsequent path is obtained from the incremental equilibrium equation [eqn (40) with b replaced by η from eqn (45)]. It falls to a minimum at $p = 1.37$, $\theta = 0.78$ and $\phi = 0.37$, and then rises. Therefore, if p is increased beyond $p = 1.44$, the system snaps to point B, where $p = 1.44$, $\theta = 1.12$ and $\phi = 0.62$, and then follows the stable rising path, with the spring length fixed at 0.6 L [from eqn (45)].

In Fig. 8, $\theta = 0.05$ when $p = 0$. As p is increased, the bar rotates smoothly until the spring reaches 0.6 L, which occurs at $p = 1.32$, $\theta = 0.57$ and $\phi = 0.24$ (point A). The subsequent path is unstable until its minimum at $p = 1.30$, $\theta = 0.73$ and $\phi = 0.33$. If p is increased beyond the transition point A, the system snaps to point B, where $p = 1.32$, $\theta = 0.91$ and $\phi = 0.45$, and then the friction element slips as θ increases further.

6. EXAMPLE 4: ELASTIC BAR WITH FRICTION ELEMENT AT TIP

In this example, the bar is not rigid in the axial direction, but is elastic with stiffness k and tip deflection w (positive for compression). Also, the friction element is attached to the bar at its tip, and has negligible dimensions (i.e. the tip of the bar is in contact with the friction plane). The configuration of the system is shown in Fig. 9(a) before slip is activated and in Fig. 9(b) during slip. As before, u_x and u_y are the horizontal and vertical deflections, respectively, of the element. The forces acting on the element during slip are depicted in Fig. 9(c), with S representing a shear force.

There is no deflection of the system (i.e. $\theta = \delta$, $w = 0$) until slip is activated. During slip, $\bar{n} = m = 2$, $q_1 = \theta$, $q_2 = w$ and a_1, a_2, T_1, T_2 and λ are given in eqns (30). The potential energy is

$$V = (c/2)(\theta-\delta)^2 - P[L\cos\delta - (L-w)\cos\theta] + (k/2)w^2 \tag{51}$$

and the dissipation function is the same as in eqn (46). From geometry,

$$u_x = (L-w)\sin\theta - L\sin\delta, \quad u_y = L\cos\delta - (L-w)\cos\theta, \tag{52}$$

leading to the rates

$$\dot{u}_x = (L-w)\dot{\theta}\cos\theta - \dot{w}\sin\theta, \quad \dot{u}_y = (L-w)\dot{\theta}\sin\theta + \dot{w}\cos\theta. \tag{53}$$

Equations (53) are substituted into eqn (46), and eqns (16) then yield the following equilibrium equations:

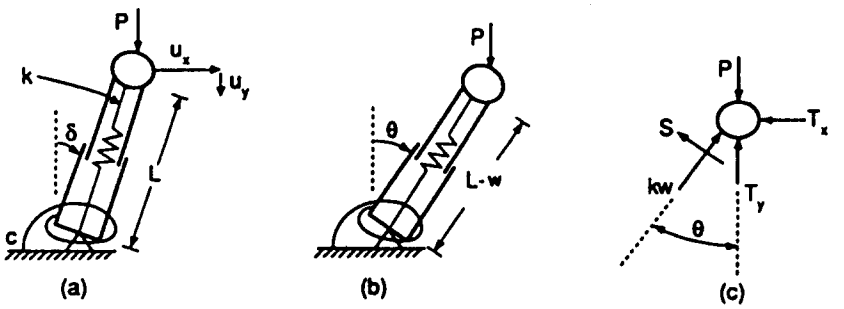

Fig. 9. Geometry of Example 4: (a) before slip; (b) during slip; (c) forces on friction element during slip.

$$c(\theta-\delta)-(L-w)[(P-T_y)\sin\theta-T_x\cos\theta]=0, \tag{54}$$

$$kw-(P-T_y)\cos\theta-T_x\sin\theta=0. \tag{55}$$

Using $\theta=\delta$ and $w=0$ in eqns (54) and (55), and the limit friction condition in eqn (12) leads to the values $T_x=0$, $T_y=T_0$ and $P=T_0$ when slip is activated.

The incremental forms of eqns (54) and (55) are

$$c\dot\theta-(L-w)[(\dot P-\dot T_y+T_x\dot\theta)\sin\theta+(P\dot\theta-T_y\dot\theta-\dot T_x)\cos\theta]$$
$$+\dot w[(P-T_y)\sin\theta-T_x\cos\theta]=0, \tag{56}$$

$$k\dot w+(P\dot\theta-T_y\dot\theta-\dot T_x)\sin\theta-(\dot P-\dot T_y+T_x\dot\theta)\cos\theta=0. \tag{57}$$

Differentiation of the limit friction condition in eqn (12) yields the relation

$$T_x\dot T_x+T_y\dot T_y=0. \tag{58}$$

Also, substitution of eqns (53) into the slip rule (31) gives

$$(L-w)(T_x\sin\theta-T_y\cos\theta)\dot\theta-(T_x\cos\theta+T_y\sin\theta)\dot w=0. \tag{59}$$

Equations (56)–(59) are linear equations in the rates $\dot P$, $\dot T_x$, $\dot T_y$, $\dot w$ and $\dot\theta$. One can start from the slip activation point, with $P=T_0$, $T_x=0$, $T_y=T_0$, $\theta=\delta$ and $w=0$, and apply these four equations to develop the deformation path. For example, one can select a small value for $\dot\theta$, solve the linear equations for the other four rates, and then add these five increments to the corresponding values to get the next state of the system. Its accuracy can be checked by substituting the values of P, T_x, T_y, w and θ into the equilibrium equations (54) and (55). Alternatively, one can manipulate eqns (54)–(59) and eliminate some of the variables. In the numerical examples to follow, for instance, $\dot T_y$ and $\dot w$ were eliminated, $\dot\theta$ was specified and two simultaneous equations were solved for $\dot P$ and $\dot T_x$.

In this example, the non-dimensional quantities are defined by

$$p=P/(kL),\quad t_0=T_0/(kL),\quad \varepsilon=c/(kL^2),\quad \bar w=w/L, \tag{60}$$

and results are obtained for $\delta=0.1$, $t_0=0.001$ and $\varepsilon=0.001, 0.005$ and 0.010. Deformation paths are plotted in the θ, p plane in Fig. 10. Slip is activated at $p=0.001$, $\theta=0.1$ and $\bar w=0$. Rising portions of the path are stable and falling portions are unstable. For the case $\varepsilon=0.001$, a maximum occurs at $p=0.0094$, $\theta=0.109$ and $\bar w=0.0092$, and further increase

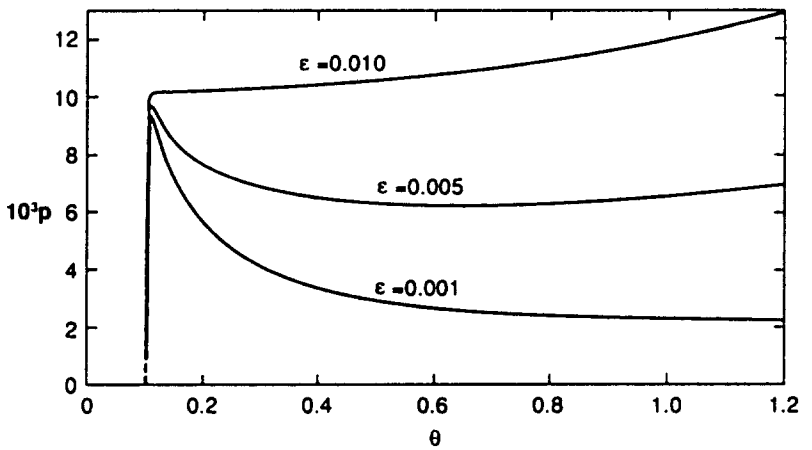

Fig. 10. Load–displacement curves in the θ, p plane for Example 4 when $\delta=0.1$ and $t_0=0.001$.

in p leads to a dynamic snap. The path has a minimum at $p = 0.0023$, $\theta = 1.114$ and $\bar{w} = 0.0010$. When $\varepsilon = 0.005$, a maximum occurs at $p = 0.0097$, $\theta = 0.110$ and $\bar{w} = 0.0096$, and there is a minimum at $p = 0.0062$, $\theta = 0.639$ and $\bar{w} = 0.0050$. Finally, if $\varepsilon = 0.010$, there is a slight snap from $\theta = 0.115$ to $\theta = 0.121$ when $p = 0.0102$, and for larger values of ε the limit points will disappear and the entire path will be rising and stable.

Acknowledgements—The authors are grateful to C.-C. Cheng for carrying out the numerical computations. They also thank the reviewers for helpful suggestions.

REFERENCES

Hoff, N. J. (1949). Dynamic criteria of buckling. In *Engineering Structures*, pp. 121–139. Academic Press, New York.

Huseyin, K. (1975). *Nonlinear Theory of Elastic Stability*. Noordhoff, Leyden, The Netherlands.

Kerr, A. D. (1973). A model study for vertical track buckling. *High Speed Ground Transp. Jl* 7, 351–368.

Klepp, H. J. (1990). Migration of the oscillation centre inside equilibrium zones. *J. Sound Vib.* **138**, 193–204.

Martins, J. A. C., Oden, J. T. and Simões, F. M. F. (1990). A study of static and kinetic friction. *Int. J. Engng Sci.* **28**, 29–92.

Michałowski, R. and Mróz, Z. (1978). Associated and non-associated sliding rules in contact friction problems. *Arch. Mech.* **30**, 259–276.

Oden, J. T. and Martins, J. A. C. (1985). Models and computational methods for dynamic friction phenomena. *Comp. Meth. Appl. Mech. Engng* **52**, 527–634.

Pierre, C., Ferri, A. A. and Dowell, E. H. (1985). Multi-harmonic analysis of dry friction damped systems using an incremental harmonic balance method. *J. Appl. Mech.* **52**, 958–964.

Thompson, J. M. T. and Hunt, G. W. (1973). *A General Theory of Elastic Stability*. John Wiley, New York.